

## CHAPTER V

## RESULTS AND DISCUSSIONS

5.1 Introduction

Results of the four experiments presented in the previous chapter are summarized here. The short-circuit current density,  $J_{sc}$  given here is approximately equal to the photocurrent density,  $J_{ph}$  by considering that series resistance,  $R_s$  becomes less important at low intensities. Hence, the diode dark current is negligible as compared to the photocurrent. Furthermore, the shunt current is also negligible.

5.2 Results and Discussions of Group I solar cells

Results of the group I solar cells are summarized in Fig.37 and Table 6.

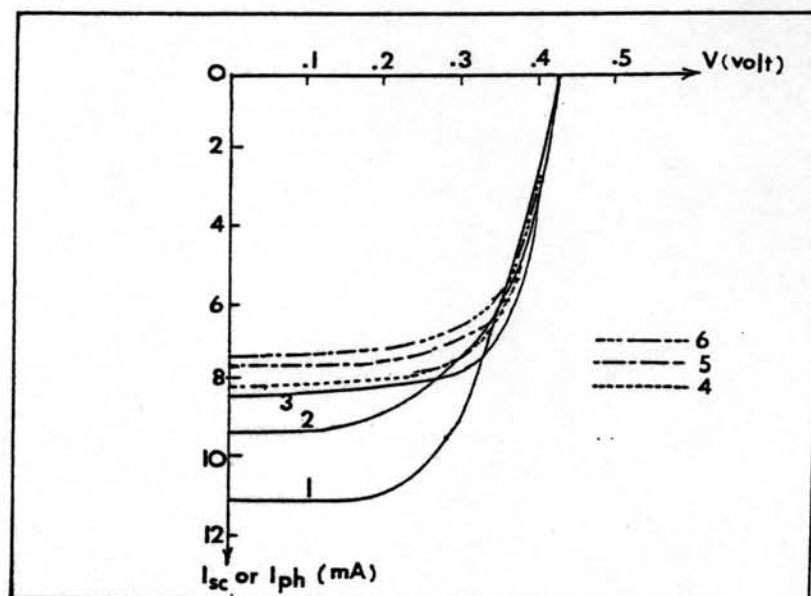


Fig.37 the I-V characteristic solar cell curves with different junction depths. The illuminated area of each cell is  $0.68 \text{ cm}^2$  and the temperature is  $40^\circ\text{C}$ .

Summary of Experimental Internal Parameters of Group I Solar Cells: AM1.

Solar Cell number	$x_j$ ( $\mu\text{m}$ )	$J_{sc}$ or $J_{ph}$ ( $\text{mA}/\text{cm}^2$ )	$V_{oc}$ (Volts)	FF	Efficiency (%)	$R_s$ ( $\Omega$ )	$R_{sh}$ ( $\text{K}\Omega$ )	n	$I_s$ ( $\text{A}/\text{cm}^2$ )	sheet Resistivity ( $\Omega/\square$ )
1	0.28	16.2	0.42	0.57	3.9	6.0	2.0	1.42	$1.76 \times 10^{-7}$	10.8
2	0.49	13.5	0.42	0.60	3.4	0.5	8.5	2.56	$2.39 \times 10^{-5}$	7.5
3	0.60	12.4	0.42	0.69	3.6	0.6	5.5	1.44	$1.58 \times 10^{-7}$	6.0
4	0.71	12.1	0.42	0.68	3.4	1.5	5.1	1.54	$3.20 \times 10^{-7}$	3.4
5	1.05	11.5	0.42	0.62	3.0	0.4	7.2	1.68	$7.35 \times 10^{-7}$	3.1
6	1.34	11.0	0.42	0.69	2.9	1.0	5.1	2.20	$8.23 \times 10^{-6}$	2.9

Table 6

Fig. 37 and Table 6 show that the photocurrent densities decrease because of the increase in junction depth of diffused layer as numerically predicted in section 3.6.1 of chapter IV. On the other hand, for deeper junctions, the photocurrent decreases because of reduction in collection of minority carriers. However, since the current flows laterally to the contacts in the diffused layer, the junction depth should not be made too shallow. By designing the optimum of separation and width of the grid strips of the front contact, this effectively reduces the resistance of the diffused layer. And the junction depth can be made shallower to increase the number of carriers crossing the junction.

### 5.3 Results and Discussions of Group II Solar Cells.

Results of the group II solar cells are summarized in Fig.38 and Table 7

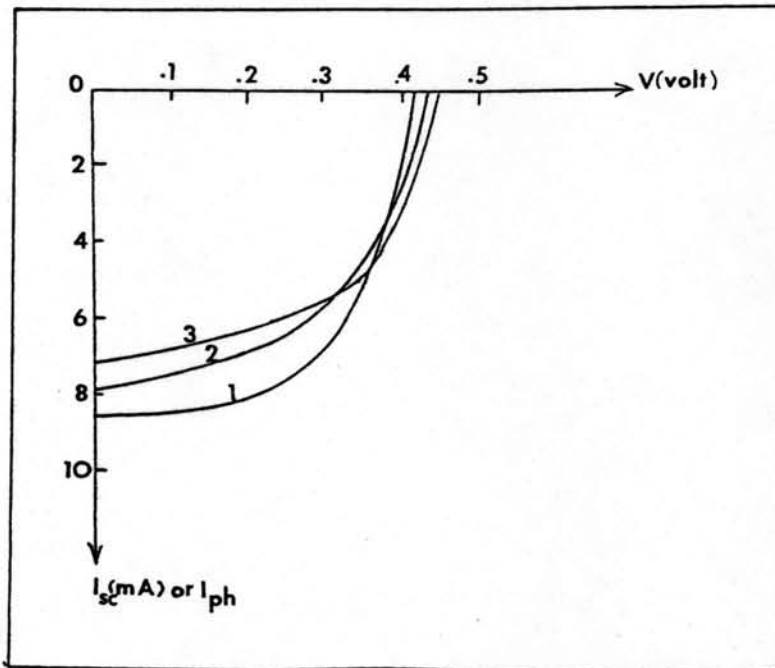


Fig. 38 The I-V characteristic solar cell curves with different substrate resistivities. The illuminated area of each cell is  $0.344 \text{ cm}^2$  and the temperature is  $40^\circ\text{C}$ .

Curves 1,2 and 3 represent substrate resistivities of 23,17 and  $1.9 \Omega\text{-cm}$  respectively. Each of the cells has a junction depth of  $0.5 \mu\text{m}$ .

Fig.38 and Table 7 show that at high substrate resistivities, the photocurrent densities increase as explained in section 3.6.3 of chapter III. It can be noticeable that low resistivities result in a high open-circuit voltage because of the reduction in dark current as can be seen in Fig.39 and simple equation below.

Summary of Measured Internal Parameters of Group II Solar Cells: AM1

Solar Cell number	$\rho_b$ ( $\Omega$ -cm)	Junction Depth ( $\mu\text{m}$ )	$J_{sc}$ or $J_{ph}$ ( $\text{mA}/\text{cm}^2$ )	$V_{oc}$ (Volts)	FF	Efficiency (%)	$R_s$ ( $\Omega$ )	$R_{sh}$ (K )	Ideality Factor, n	$I_s$ ( $\text{A}/\text{cm}^2$ )	Sheet Resistivity ( $\Omega/\square$ )
1	1.9	0.5	19.8	0.44	0.55	4.79	1	0.5	2.9	$5.4 \times 10^{-5}$	2.8
2	10	0.5	24.4	0.43	0.59	5.68	2.5	4.6	2.4	$2.4 \times 10^{-5}$	4.4
3	17	0.5	22.7	0.42	0.58	5.53	2	0.45	2.9	$8.2 \times 10^{-5}$	*

\* unmeasurable

Table 7

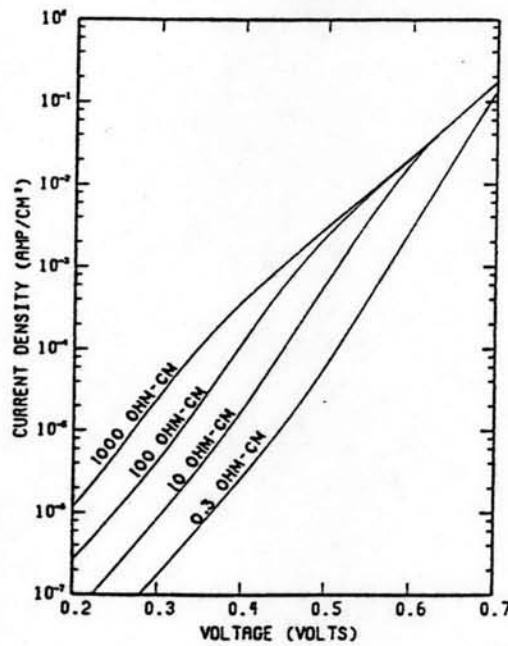


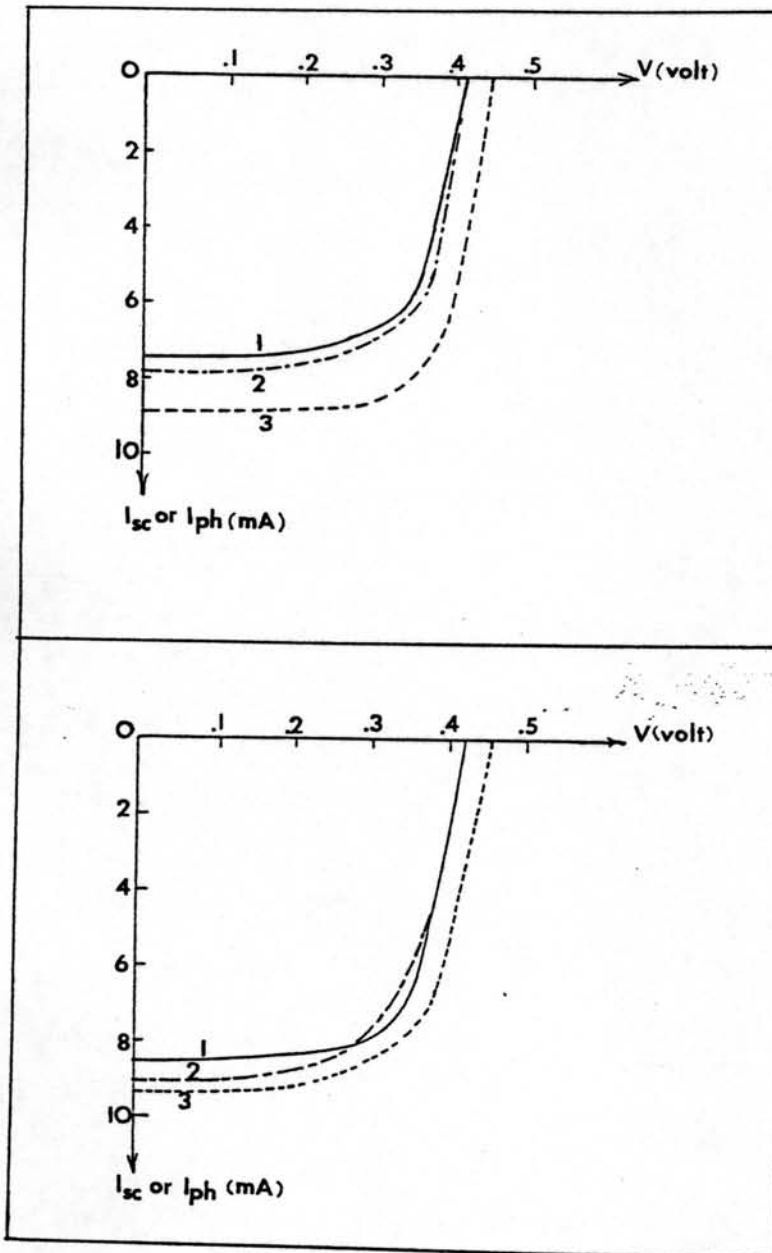
Fig.39 Dark J-V characteristics for solar cells of various base layer.<sup>(9)</sup>

$$V_{oc} = nV_T \ln\left(\frac{I_{sc}}{I_s} + 1\right) \quad (28)$$

where  $I_s$  is the dark or reverse saturation current and  $V_T$  is the thermal voltage. It can be noticed here that the high values of  $n$  are due to the internal field emission taking place in extremely narrow space charge region in n-p junctions.<sup>(5,19)</sup> The shunt resistances are low because it takes too long time for contact sintering.

### 5.4 Results and Discussions of Group III Solar Cells.

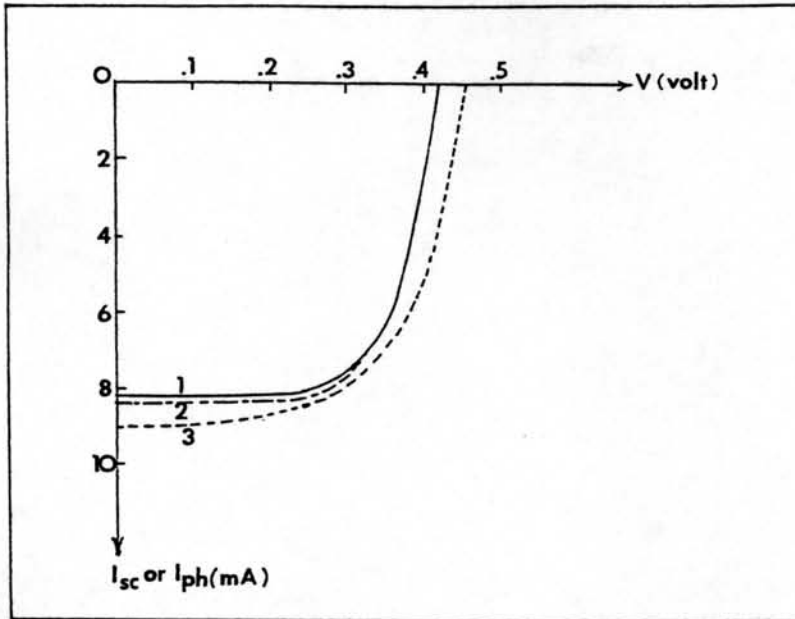
Results of peeling-off the surface of the cells using the anodic oxidation technique are shown in Fig.40 Table 8.



1.  $x_j = 1.34 \mu\text{m}$
2.  $x_j = 1.05 \mu\text{m}$
3. After the top surface being peeled-off  $0.29 \mu\text{m}$  thick, and the new  $x_j$  is  $1.05 \mu\text{m}$ .

1.  $x_j = 0.6 \mu\text{m}$
2.  $x_j = 0.49 \mu\text{m}$
3. After the top surface being peeled-off  $0.11 \mu\text{m}$  thick and the new  $x_j$  is  $0.49 \mu\text{m}$

Fig.40



1.  $x_j = 0.71 \mu\text{m}$
2.  $x_j = 0.6 \mu\text{m}$
3. After the top surface being peeled-off  $0.11 \mu\text{m}$  thick and the new  $x_j$  is  $0.6 \mu\text{m}$ .

Fig.40 The I-V characteristic solar cell curves show the effect of peeling-off the top surface of the cells by means of anodic oxidation.

Summary of Fabrication of Solar Cells with Peeled-Off the Top Surface by means of Anodic Oxidation:AM1.

Solar Cell number	$x_j$ ( $\mu\text{m}$ )	Jsc or Jph ( $\text{mA}/\text{cm}^2$ )	Voc (Volts)	FF	Efficiency (%)
3	0.60	12.4	0.42	0.69	3.5
3*	0.49	13.8	0.45	0.63	3.9
2	0.49	13.5	0.42	0.60	3.4

Table 8



Solar Cell number	$x_j$ ( $\mu\text{m}$ )	Jsc or Jph ( $\text{mA}/\text{cm}^2$ )	Voc (Volts)	FF	Efficiency (%)
4	0.71	12.0	0.42	0.68	3.4
4*	0.60	13.2	0.45	0.62	3.7
3	0.60	12.4	0.42	0.69	3.6

Solar Cell number	$x_j$ ( $\mu\text{m}$ )	Jsc or Jph ( $\text{mA}/\text{cm}^2$ )	Voc (Volts)	FF	Efficiency (%)
6	1.34	10.0	0.42	0.69	2.9
6*	1.05	12.9	0.45	0.62	4.0
5	1.05	11.5	0.42	0.69	3.0

Table 8

The three I-V characteristics of solar cells show that peeling-off the top surface of solar cells by means of anodic oxidation result in a higher short-circuit current or photocurrent densities, and most significantly the open-circuit voltage. Even when they are compared to the solar cell with the same junction.

A higher short-circuit current or photocurrent is due to the reduction in junction depth. The reduced junction depth employed here is to minimize the heavily damaged layer or dead layer which occurs at the top surface of  $n^+$  diffused region (around  $1000\text{\AA}$  adjacent to the top surface). Photocarriers can not be collected from this layer because of such a short lifetime (or very high front surface recombination velocity)

here (less than 100 ps).<sup>(10)</sup> Therefore, solar cells with peeled-off the top surfaces reduce the recombination losses in the top region.

A higher open-circuit voltage,  $V_{oc}$ , is due to the reduced recombination losses which results in the lower effective front surface recombination velocity. This front surface recombination velocity is a strong function of open-circuit voltage as is shown in Fig.41<sup>(17)</sup>

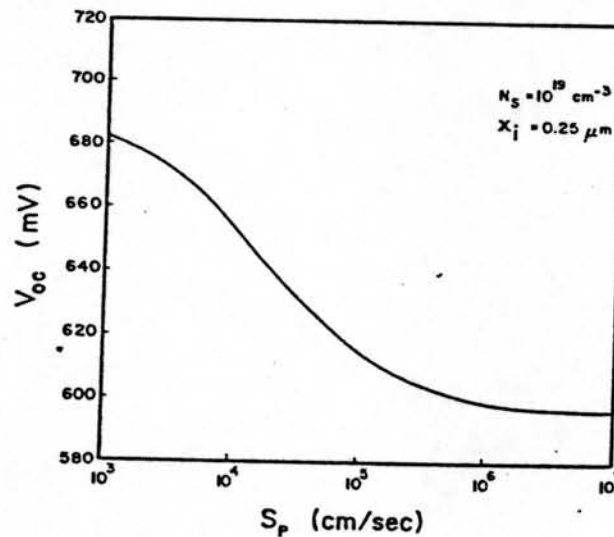


Fig.41 Calculated dependence of  $V_{oc}$  on the front surface recombination velocity,  $S_p$ , for an  $n^+$ -p silicon solar cell with a transparent emitter.<sup>(17)</sup>

Therefore, Solar cells with peeled-off the top layer result in a higher performance (see Table 8).

### 5.5 Results and Discussions of Group IV Solar Cells

The Back Surface Field (BSF) effect on a conventional n-on-p silicon solar cell or  $n^+$ -p-p<sup>+</sup> structure results in a higher performance than an ordinary n-on-p solar cell. This is shown in Fig.42 and Table 9.

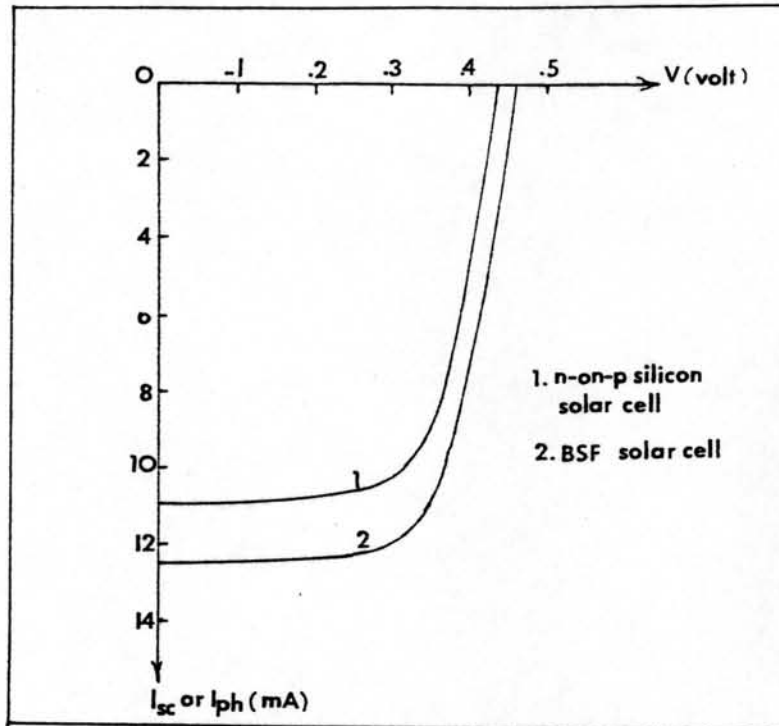


Fig.42 The experimental curves of an BSF compares to an n-on-p silicon solar cell. Substrate resistivities of both solar cells are  $23.7 \Omega\text{-cm}$  (or diffusion length of  $245 \mu\text{m}$ ) and  $200 \mu\text{m}$  thick.

Summary of the Experimental Value Comparison Between BSF and Ordinary n-on-p Silicon Solar Cells: AM1.

BSF	Jsc ( $\text{mA}/\text{cm}^2$ )	Voc (Volts)	FF	Efficiency (%)	Front Junction Depth, ( $\mu\text{m}$ )	Back Junction Depth, ( $\mu\text{m}$ )
No	10.9	0.43	0.689	3.2	1.0	-
Yes	12.3	0.45	0.699	3.87	1.0	1.05

Table 9

The short-circuit current or photocurrent density is increased by the BSF effect as shown in Fig.42, and the experimental values comparison between with and without BSF is given in the Table 9. The current is increased due to the fact that loss of minority carriers is reduced at the back surface of the cell. The loss of minority carriers is reduced because the addition of the back surface built-in electric field which opposes the motion of electrons to the back surface, can result in an effective back surface recombination velocity which is much lower than the actual back surface recombination velocity<sup>(18)</sup>.

The increase in open-circuit voltage are due to a combination of three factors. Firstly, the increase in short-circuit current,  $I_{sc}$ , which was mentioned above. Secondly, a decrease in the diode dark current,  $I_s$ , (or the diode leakage current) due to reduced recombination at the back surface of electrons injected from the  $n^+$  region into the base. Finally, a modulation of the barrier,  $\psi_p$ , as shown in Fig.44 by the change in minority carriers densities at high-low junction edge, that is, when the cell is open-circuited.

The base region width should be less than the diffusion length,  $L_n$ , so that the full effect of the  $p-p^+$  junction is then realized<sup>(16)</sup>.

In conclusion,BSF solar cells have a higher performance than ordinary solar cells.

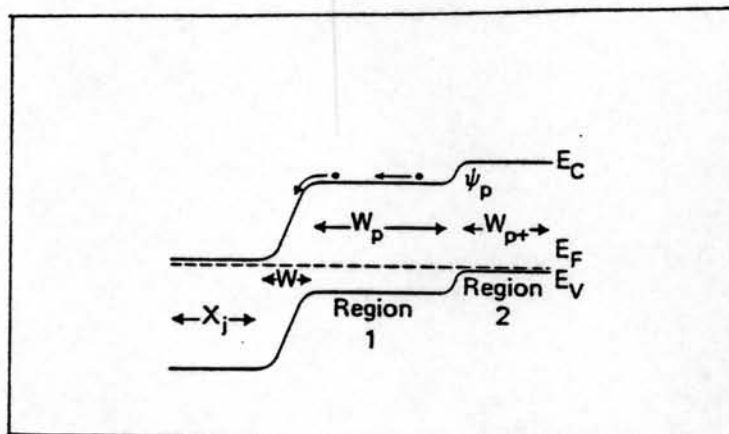


Fig.43 Energy band diagram of a BSF (blocking back contact) device<sup>(1)</sup>.